Polymer Chemistry

ROYAL SOCIETY OF CHEMISTRY

PAPER

View Article Online
View Journal | View Issue



Cite this: *Polym. Chem.*, 2024, **15**, 1399

# A versatile modification strategy to enhance polyethylene properties through solution-state peroxide modifications†

Utku Yolsal,[a] Thomas J. Neal,[a] James A. Richards,[b] John R. Royer[b] and Jennifer A. Garden *[a]

Polymers with high molecular weights have superior properties, such as enhanced impact and chemical resistance. While these properties can be achieved by converting a thermoplastic into a thermoset, this can prevent polymers from further processing as thermosets cannot be melted and moulded without damaging their internal structure. Therefore, increasing the molecular weight of a polymer without losing the ability to process it is of utmost importance. Polyethylene (PE), the most commonly produced plastic in the world, is comprised of strong C–C and C–H bonds, which makes its controlled chain extension challenging to achieve. Herein, we report a novel, solution-based method for the modification of PE chains using commercially available, low-cost organic peroxides in solvents such as dichlorobenzene and *tert*-butylbenzene. To the best of our knowledge, this is the first solution-based methodology for PE modification through the incorporation of long chain PE branches by using organic peroxides. The effects of the modification reactions were extensively investigated using rheology, differential scanning calorimetry, small/wide angle X-ray scattering, size exclusion chromatography and NMR spectroscopy, and model studies were performed with *n*-dodecane to confirm the formation of branched moieties. The enhanced mechanical properties of the materials were demonstrated using rheology, where the modified polymers show significantly increased stiffness and higher viscosities. This is attributed to reactions between the PE chains to form branched structures, thus increasing both the molecular weight of the feedstock and the number of entanglements within the polymer microstructure. This methodology enables the properties of PE to be tailored, providing a shortcut for the development of new PE grades and formulations as its applications continue to grow in developing technologies such as 3D printing, artificial joints and soft robotics.

Received 21st December 2023,
Accepted 15th February 2024

DOI: 10.1039/d3py01399e

rsc.li/polymers



## Introduction

Increasing the molecular weight of a molecule leads to remarkable enhancements in its physical and mechanical properties.[1–3] The typical progression is from monomer to oligomer, then to polymer and ultimately to pleistomer, a word coined by Simionescu *et al.* for 'very many parts'.[4] Nowadays, the term "ultra-high molecular weight polymers" is more frequently used.[5] Polymers with enhanced mechanical properties, such as superior impact and chemical resistance, are desirable for many everyday materials.[6,7] While there are numerous methods of achieving these properties,[8] they often rely on crosslinking strategies which can convert thermoplastics into thermosets. As thermosets cannot be melted and/or remoulded without damaging their internal structures,[9] these methods can have detrimental effects on the polymer processability. Therefore, developing strategies to increase the molecular weights of polymer chains, whilst avoiding crosslinking, is of paramount importance.

Polyethylene (PE) accounts for one third of the entire plastics markets,[10] and has many applications as a high performance speciality polymer, including developing technologies such as implantable medical devices and advanced composites.[11–13] The properties of PE can be modified during its synthesis, through careful choice of the initiator, and PE can also be modified post-synthesis, traditionally through reactive extrusion at high temperatures to achieve grafting on the PE surface.[14–16] For example, the grafting of maleic anhydride can improve the polymer's adhesive properties.[17,18] As the PE surface is made up of strong C–C and C–H bonds, it is usually necessary to use high-energy species to modify polyethylene,

[a]*EaStCHEM School of Chemistry, University of Edinburgh, Joseph Black Building, David Brewster Road, Edinburgh, EH9 3FJ Scotland, UK. E-mail: j.garden@ed.ac.uk*
[b]*School of Physics and Astronomy, University of Edinburgh, King's Buildings, Peter Guthrie Tait Road, Edinburgh, EH9 3FD Scotland, UK*

† Electronic supplementary information (ESI) available. See DOI: https://doi.org/10.1039/d3py01399e

and a number of industrial processes already use radical-releasing peroxides.[19,20] The organic peroxides employed are specifically chosen to be stable at room temperature and decompose when heated to PE extrusion temperatures, rapidly releasing radicals that react with the usually inert PE surface to form macroradicals. The macroradicals can subsequently undergo a variety of different reactions to modify the polymer chains (Scheme 1).[21,22]

The reaction of PE with organic peroxides often leads to the formation of long chain branching (LCB) on the polymer chains. In LCB the side chains are over twice the molecular entanglement weight, and both the backbone and sidechains are entangled.[23] Therefore, even a small component of LCB polymers can have a significant effect on the mechanical properties and improve the end properties.[24–27] This arises from an increase in extensional strain hardening, *e.g.*, preventing film rupture, while maintaining a low high-shear viscosity.[28] Melt-state PE modifications with peroxides are already used in some commercial processes, yet this can generate polymers with gel fractions due to the poor dispersion of the organic peroxides.[24,29] This can be attributed to poor mixing of the organic peroxide in the viscous polymer melt, resulting in "pockets" of radicals where certain parts of the polymer become highly cross-linked whilst others are sparsely modified. Solution-state modifications of PE have the potential to tackle some of the issues associated with the melt-state PE/peroxide modifications, by ensuring homogeneous LCB without introducing crosslinks into the polymer microstructure. Yet compared to the melt-state, solution-state modifications of PE are significantly underexplored. This is likely due to the challenge of modifying the strong C–C and C–H bonds of PE whilst avoiding competitive reactions with the solvent; this is especially difficult considering the solubility challenge associated with the crystallinity of high-density PE (HDPE).

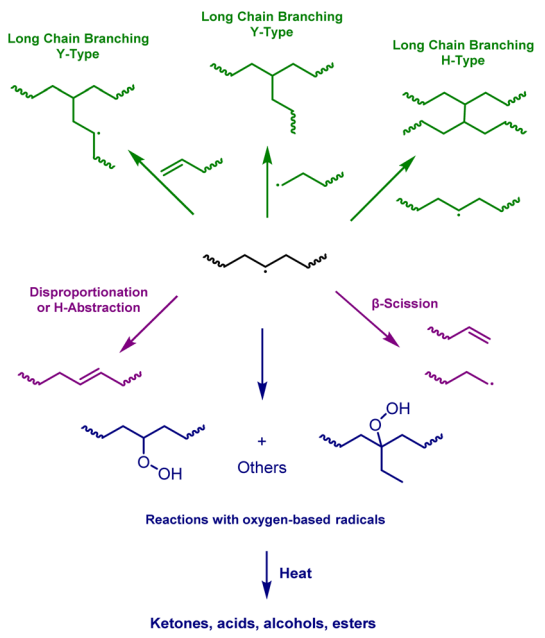


**Scheme 1** A simplified reaction map for the post-polymerisation modification of PE from a generated macroradical.

To the best of our knowledge, solution-based peroxide modifications of PE have focussed on grafting,[30,31] and polymer enhancements through LCB have not been explored. Herein, we report an unprecedented solution-state peroxide modification method for PE that can be used to enhance the material properties through LCB, and can alter the feedstock grade from an injection-moulding grade into a blow-moulding grade material.

## Results and discussion

### Solution-state peroxide modification

Modification reactions were performed on a commercially available injection-moulding grade HDPE (IMPE). This polymer was extensively characterised using $^{1}$H and $^{13}$C NMR spectroscopy prior to the modification reactions to fully understand the composition and microstructure (Fig. S1–4†). The NMR analysis revealed that the polymer largely consisted of ethylene repeats units but also contained a small number of ethyl branches, arising from a 1-butene comonomer at an estimated 1.2 mol% loading (Calculation S1†). End group analysis was also performed by $^{1}$H NMR spectroscopy (Fig. S4†), which showed that most chains are fully saturated with the majority of end groups being $CH_3$ units, with a near absence of olefinic end groups.[32,33] Aromatic protons of low intensity were also observed in the $^{1}$H NMR spectrum of IMPE. As this is a commercial grade sample, it was assumed to contain additives, such as antioxidants and light stabilisers in-line with industry standards. The NMR signals are likely to be attributed to these additives, which are often phenolic species.[34] While it is known that antioxidant additives can slow down the cross-linking process initially, they lose their effectiveness in the presence of organic peroxides as the modification reactions continue.[35–37] Given that the study targets altering grades of commercial polymers, the samples were used as received, to understand the effectiveness of the organic peroxides.

Initially, a range of different conditions were tested to find the optimal conditions for the modification reactions. As HDPE is a highly crystalline polymer, heat was essential to dissolve the polymer in an organic solvent, which disrupts the crystalline domains. HDPE is commonly dissolved in high boiling point aromatic hydrocarbons or in halogenated solvents.[20] As organic peroxides decompose to release radicals, we targeted solvents that would not compete with polyethylene C–H groups for hydrogen abstraction. This was particularly important as polymer concentrations of <10 w/v% were used, due to the viscosity of HDPE solutions. Dichlorobenzene (DCB) was selected as the main solvent for the initial investigations due to the decreased stability of $sp^2$ radicals *vs.* $sp^3$ radicals, which was expected to disfavour C–H abstraction from the solvent molecules compared to the $CH_2$ units on PE. A range of other solvents were also studied to investigate compatibility with the organic peroxide modifications, including *tert*-butylbenzene (TBB), *n*-nonane and anisole.

Dilauroyl peroxide (DLP) and benzoyl peroxide (BPO) were both chosen as suitable organic peroxides. Dicumyl peroxide (DCP) and 2,5-bis(*tert*-butylperoxy)-2,5-dimethylhexane (BDH) are typically used for melt-phase PE modifications because they decompose rapidly at the extrusion temperatures (170–190 °C) with short half-times (<2 min).[38,39] However, it was hypothesised that the reduced viscosity in solvent compared to the melt state would enable lower reaction temperatures to be used, and thus reaction temperatures in the range of 125–135 °C were selected as being well below the solvent boiling points. Therefore, DLP and BPO were selected for this temperature range because, at 125 °C, the half-life values were predicted to be 0.45 and 1.9 min in chlorobenzene, respectively.[40]

Following dissolution of HDPE in DCB at 125 °C, a solution of the peroxide in DCB was added to the polymer solution over a period of time (usually 20 min) and the reaction solution was stirred for a further 20 min (Scheme 2 and Table 1). All polymers were recovered by precipitation in hexane, and were filtered and dried before further characterisation (refer to Experimental for further details). A range of different conditions were tested to understand how each variable affects the modification reactions. Initial experiments were performed using DLP, and the peroxide loading was varied from 0 to 6 wt% relative to the polymer weight. All polymers remained fully soluble during and after the modification reactions, indicating that no crosslinks were introduced.

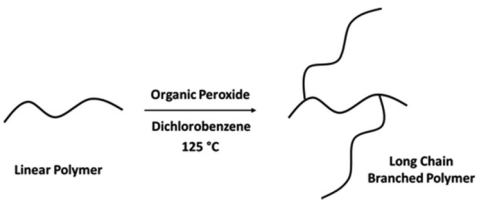


**Scheme 2** Solution-state modification of HDPE using organic peroxides.

**Table 1** Experimental conditions for the solution-state modification reactions. All reactions were performed under inert atmosphere for 20 min following the addition of the peroxide solution[a]

| Exp. | Peroxide | Peroxide Loading (wt%) | Solvent | Peroxide addition duration (min) |
|---|---|---|---|---|
| **M1** | Control | 0 | DCB | 20 |
| **M2** | DLP | 1.5 | DCB | 20 |
| **M3** | DLP | 3.0 | DCB | 20 |
| **M4** | DLP | 4.5 | DCB | 20 |
| **M5** | DLP | 6.0 | DCB | 20 |
| **M6** | DLP | 4.5 | TBB | 20 |
| **M7** | DLP | 4.5 | *n*-Nonane | 20 |
| **M8** | DLP | 4.5 | Anisole | 20 |
| **M9** | DLP | 3.0 | DCB | 6 |
| **M10** | DLP | 3.0 | DCB | 1 |
| **M11** | DLP | 3.0 | DCB | 0.02 |
| **M12** | DLP[b] | 4.5 | DCB | 20 |
| **M13** | Dried BPO | 1.0 | DCB | 20 |
| **M14** | Dried BPO | 2.0 | DCB | 20 |
| **M15** | Dried BPO | 3.0 | DCB | 20 |
| **M16** | Dried BPO | 3.0 | TBB | 20 |
| **M17** | Wet BPO | 3.0 | DCB | 20 |
| **M18** | Wet BPO | 3.0 | TBB | 20 |
| **M19** | Wet BPO[c,d] | 0.5 | DCB | 20 |
| **M20** | Wet BPO[d] | 0.5 | DCB | 20 |

[a] All reactions were performed at 125 °C, at 7.5 w/v% polymer concentration, under inert atmosphere unless otherwise stated. The experiment time was 20 min after the peroxide addition. [b] The reaction was performed at 135 °C. [c] The reaction was performed under air, instead of inert atmosphere. [d] The polymer concentration was 5 w/v%.

### Characterisation of the PE properties and structure

Oscillatory melt rheology was performed to understand how the dynamic mechanical properties and the underlying polymer properties of the starting feedstock changed following the peroxide modifications (Fig. 2). Under small amplitude oscillatory shear, storage ($G'$) and loss ($G''$) moduli, representing elastic and viscous responses can be obtained as a function of angular frequency ($\omega$). These can also be represented through the complex modulus ($|G^*| = \sqrt{(G'^2 + G''^2)}$) or viscosity ($|\eta^*| = |G^*|/\omega$) and phase angle ($\delta = \tan^{-1} G''/G'$). The complex viscosity is of practical use, as it can be related to the steady-shear viscosity, of relevance during processing, *via* the empirical Cox–Merz rule, $|\eta^*|(\omega) = \eta$.[41]

To provide a benchmark for the modification reactions, the rheological properties of IMPE were characterised. The tests were performed using a parallel-plate geometry, which restricted the sample surface exposed to air, and the temperature was set to 190 °C to mimic the commercial processing temperature of HDPE. IMPE had a melt flow index (MFI) of 4 g per 10 min (190 °C, @2.16 kg). For comparative purposes, a blow-moulding grade HDPE (BMPE) was tested and had an MFI of 0.2 g per 10 min (190 °C, @2.16 kg). Altering the PE grade from injection to blow-moulding grade would validate the solution-state modification methodology for increasing the molecular weight of the starting feedstock, and thus the rheological properties of BMPE were also characterised. At 190 °C, $G''$ dominates over $G'$ at all the tested frequencies for IMPE, with $G'$ having a steeper slope than $G''$ (0.9 *vs.* 0.75). This is indicative of the terminal regime,[42] meaning that there is enough time for polymer chains to relax and diffuse through any entanglements (reptate) during the test timescales (Fig. 1 and S5–7†). However, these slopes are much weaker than expected for a linear, monodisperse polymer (2 *vs.* 1).[43] Similar deviations have been observed for commercial PE samples, indicating a broad range of relaxation timescales from polydispersity and/or non-linear polymer architecture.[28] However, a sharply different behaviour was observed with BMPE with $G' > G''$ at high frequencies and a crossover point ($G' = G''$) at 10 rad/s, which corresponds to a slower relaxation time of 0.5 seconds (also Fig. S8–11†). In addition, there was a significant increase in $G'$ values at low frequencies (0.1–1 rad/s), where it ranged from 600 to 2000 Pa for IMPE, compared to a range of 4000–10 000 Pa for BMPE. The measurement of $G'$ is considered as one of the most reliable methods to determine the elasticity of a polymer melt.[44] This indicates that there are significantly more entanglements with the blow-moulding grade polymer.

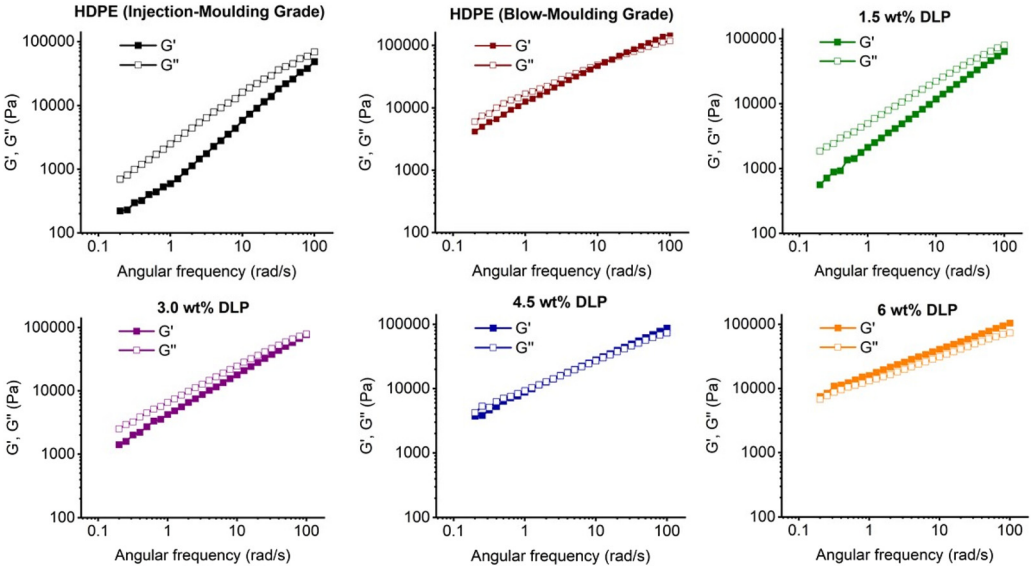


**Fig. 1** Frequency sweep experiment results obtained from the melt rheology of the model polymers and the modified samples **M1–5**.

As the dosing of DLP was increased from 0 to 6 wt%, both $G'$ and complex viscosity values of the modified IMPE samples increased significantly at low frequencies (Fig. 2 and S12–30†). In addition to 190 °C, frequency sweep tests were also performed at 140, 160 and 180 °C for **M5** (Fig. S30†), to evaluate the material properties under various processing conditions. These tests were run over 5 hours and confirmed the sample stability during the rheological measurements. This was inline with literature where it was shown that rapid oxidative changes occur at much higher temperatures (230 °C).[45] At 4.5 wt% DLP loading, the polymer viscosity profile is similar to BMPE, with a crossover frequency also observed in its frequency sweep tests. In addition, higher shear-thinning behaviours were observed with increasing DLP loadings, suggesting the presence of LCB.[46] LCB is thought to particularly increase the low-shear viscosity as entangled branches dramatically slow down the reptation of the backbone. As frequency (shear rate) increases, polymer chains start to disentangle resulting in a shear thinning behaviour. However, higher molecular weight linear polymers are also more entangled and slower reptating, as such the two polymer properties are difficult to initially distinguish from oscillatory rheology data. Therefore, empirical rules from derived quantities have been developed based upon tests on well-characterised samples and extended to industrial polymers.[28] The qualitative long chain branching index (LCBI = $1 - \delta/90°$) uses the phase angle at a given complex modulus, *e.g.*, $G^* = 2 \times 10^4$ Pa < $10^5$ Pa. With increasing DLP loading, the LCBI increases from 0.2 in injection-moulding grade PE, to 0.31 at 1.5 wt% peroxide loading, and through 0.41 at 3.0 wt% and 0.51 at 4.5 wt% to 0.58 at 6.0 wt%, where a higher LCBI indicates a greater degree of LCB, associated with extensional strain hardening. The peroxide-triggered polymer modification reactions result in random branches in a polymer sample, and this increases both the molecular weight of polymer chains and the entanglements associated with LCB. Promisingly, excellent control was also achieved over the melt flow properties of the modified samples (Fig. 2). While only a transition from injection to blow-moulding grade was desired, the results also demonstrated that the final flow properties of the polymers can be adjusted by simply altering the peroxide loading. This means that a feedstocks' grade can be tailored

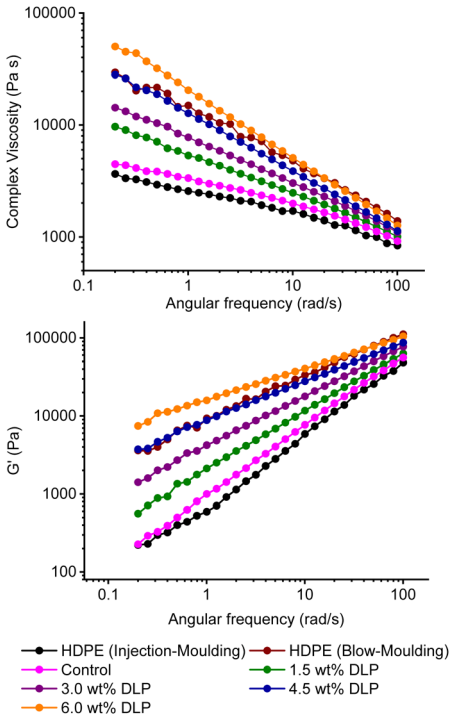


**Fig. 2** Rheological characterisation of the model injection and blow-moulding grade polymers and the samples **M1–5**.

for a particular application. It is worth noting that a control reaction performed with 0% peroxide loading also increased the complex viscosity profile of the starting feedstock, which was attributed to the removal of some lower molecular weight fractions from the sample during the precipitation steps.

The modified samples were further characterised using high temperature size exclusion chromatography (SEC) (Fig. 3 and Table 2), which was required due to the limited solubility of PE at room temperature. While the calculated number-average molecular weight ($M_n$) values remain relatively similar between the feedstock, control and the DLP modified samples, a trend can be observed with the $M_w$ and $M_p$ values, which correlate to the increased peroxide loadings. As the peroxide loadings increase from 3.0 to 4.5 and 6.0 wt% of DLP, the $M_w$ values increase from 339 to 349 and 365 kg mol$^{-1}$, respectively. In addition, investigation of the shape of the size exclusion traces shows the presence of higher molecular weight fronts at these peroxide loadings. While the $M_w$ values of the control (**M1**) and 1.5 wt% DLP samples (**M2**) appear similar, this may be due to the broad molecular weight distributions which can mask small changes in polymer sizes. Although the dispersity values are broad, ranging from 3.2 to 3.5, this is not uncommon for industrial grade polymers such as IMPE, and broad dispersities were observed for the control as well as the modified samples. The molecular weight of the highest peak ($M_p$) also shifts towards shorter retention times with increased DLP loading, confirming the increase in the polymer molecular weights. Taken together, the $M_w$ and $M_p$ values show a clear trend of chain extension with increased peroxide loading, and provide further evidence that the solution-state reactions are a successful method of modifying PE. This is attributed to the formation of macroradicals that can react with each other to form higher molecular weight polymer chains, leading to a more significant change in $M_w$ than $M_n$, as higher molecular weight chains have a greater contribution to $M_w$, giving a greater enhancement of the polymer mechanical properties.[47,48]

DSC analysis was also used to probe the changes in the modified polymer samples relative to the feedstock. HDPE is highly crystalline, due to the predominance of ethylene repeat units with minimal short chain branching and no LCB. Accordingly, **M1** (control) was found to have a crystallinity of 67.8% (refer to the ESI for additional details†). This value was determined by calculating the enthalpy change associated with melting the polymer and then by dividing this by the theoretical enthalpy of melting for a 100% crystalline PE sample (290 J g$^{-1}$).[49] As the peroxide loading increased, the crystallinity of the resulting modified polymer samples decreased in a step-wise fashion, from 67.8% (**M1**) to 63.9% (**M5**, 6 wt% DLP). This trend provides further support for the modification of the starting feedstock and also hints at the formation of long chain branches, which are known to affect the packing of PE chains and thus the crystallinity.[50,51] Taken together, the data from rheology, SEC and DSC analysis show that the solution-state modification of PE using DLP is effective and leads to an increase in polymer molecular weights. This may be due to LCB, as supported by the stronger $G'$ and complex viscosity values at low frequencies as well as the decreased polymer crystallinities.

Additionally, small-angle X-ray scattering (SAXS) and wide-angle X-ray scattering (WAXS) were performed on samples **M1**–**M5** to investigate the polymer structure and further probe the effect of DLP. In all cases, sharp peaks related to the HDPE crystal structure were observed in the WAXS pattern (Fig. S109†). The observed crystalline peaks at scattering vector ($q$) values of *ca.* 15.2 nm$^{-1}$ (0.415 nm), 16.8 nm$^{-1}$ (0.374 nm), 21.2 nm$^{-1}$ (0.296 nm) and 25.6 nm$^{-1}$ (0.245 nm) correspond to the 110, 200, 210 and 020 reflections of an orthorhombic crystalline structure characteristic of HDPE.[52–54] Additionally, a broad amorphous peak at 14.4 nm$^{-1}$ (0.436 nm) is present, highlighting the semi-crystalline nature of HDPE. The degree of crystallinity for each sample was determined by comparing the integration of the crystalline peaks with the total integration of both the crystalline and amorphous peaks (refer to the SI for additional details).[55] Similarly to DSC analysis, a general reduction in the degree of crystallinity was observed as the concentration of DLP is increased (Fig. 4). The range of crystallinity was found to be between 67.6% and 60.9%, which is concordant with the data collected by DSC. Conversely, a small increase in crystallinity was observed as the DLP content was increased from 0% to 1.5% (samples **M1** and **M2**). However, both SEC and DSC show that the peroxide influence on the polymer structure between **M1** and **M2** is subtle and thus the difference in crystallinity between these two samples may be too minor to be assessed accurately *via* WAXS analysis. A broad peak with a local maxima at *ca.* $q$ = 0.30 nm$^{-1}$ is

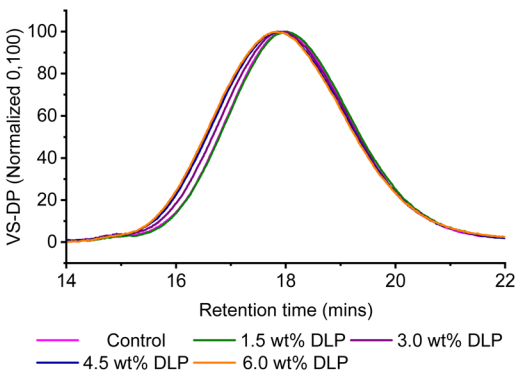


**Fig. 3** SEC viscometer traces recorded for **M1–5**, where VS-DP refers to the viscometer-differential pressure.

**Table 2** Molecular weight parameters of **M1–5** calculated using a conventional SEC calibration against polystyrene standards

| Polymer | Peroxide, loading (wt%) | $M_p$ (g mol$^{-1}$) | $M_n$ (g mol$^{-1}$) | $M_w$ (g mol$^{-1}$) | $Đ$ |
|---|---|---|---|---|---|
| **M1** | Control, 0 | 199 000 | 100 000 | 318 000 | 3.2 |
| **M2** | DLP, 1.5 | 202 000 | 87 000 | 307 000 | 3.5 |
| **M3** | DLP, 3.0 | 202 000 | 100 000 | 339 000 | 3.4 |
| **M4** | DLP, 4.5 | 211 000 | 108 000 | 349 000 | 3.2 |
| **M5** | DLP, 6.0 | 218 000 | 109 000 | 365 000 | 3.4 |

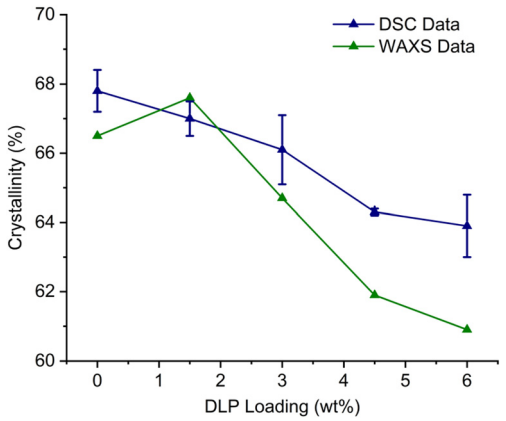


Fig. 4 A plot to demonstrate the changes in % polymer crystallinity as the peroxide loading increases.

observed in Lorenz corrected SAXS patterns of samples **M1**–**M5** (Fig. S110†) corresponding to an interlamellar spacing ($d$) of 21 nm ($d = 2\pi/q$).[56] Small variations of $d$ are observed between samples; however, these differences are extremely subtle and are likely to arise from small variations in preparation procedures between samples.

Finally, characterisation of the LCB was attempted using previously reported $^{13}$C NMR spectroscopy methods.[57–60] However, despite performing direct $^{13}$C NMR experiments over long relaxation times ($t1$ = 10 seconds) for 4k scans, it was not possible to identify any distinctive methine units originating from LCB (Fig. S112–S114†). This could be because of the broad molecular weight distribution of the polymer as well as the presence of short chain branching, which could result in sensitivity and resolution challenges where some proton environments are undetected/masked. In addition, LCB arising from the peroxide triggered modification of PE would result in either Y- or H-type branching (Scheme 1). In the near absence of olefinic end groups (as demonstrated for IMPE), peroxide-triggered modification reactions can be reasonably expected to form H-type branches *via* the reaction of two macroradicals. Identification of H-type branching is particularly challenging and, to the best of our knowledge, unequivocal $^{13}$C NMR observation of such CH–CH linking moieties has only been reported for the gamma irradiation of short *n*-alkanes or low molecular weight PE.[61–63]

Having established the concept of solution-state peroxide modification of PE, the impact of the solvent was subsequently investigated (Fig. 5). Due to the success of using DCB solvent, which features only aryl-CH protons that are challenging to abstract, TBB and anisole were also investigated, along with *n*-nonane (Fig. 5A). The chain extension reactions were performed at 4.5 wt% DLP loading, and showed a significant solvent dependence in the order DCB > TBB > anisole > *n*-nonane, as determined by the increase in complex viscosity. Interestingly, DCB is the best-performing reaction media and has no $C_{sp3}$–H units, whereas all the other solvents do. This may indicate that the alkyl groups can undergo H-abstraction,

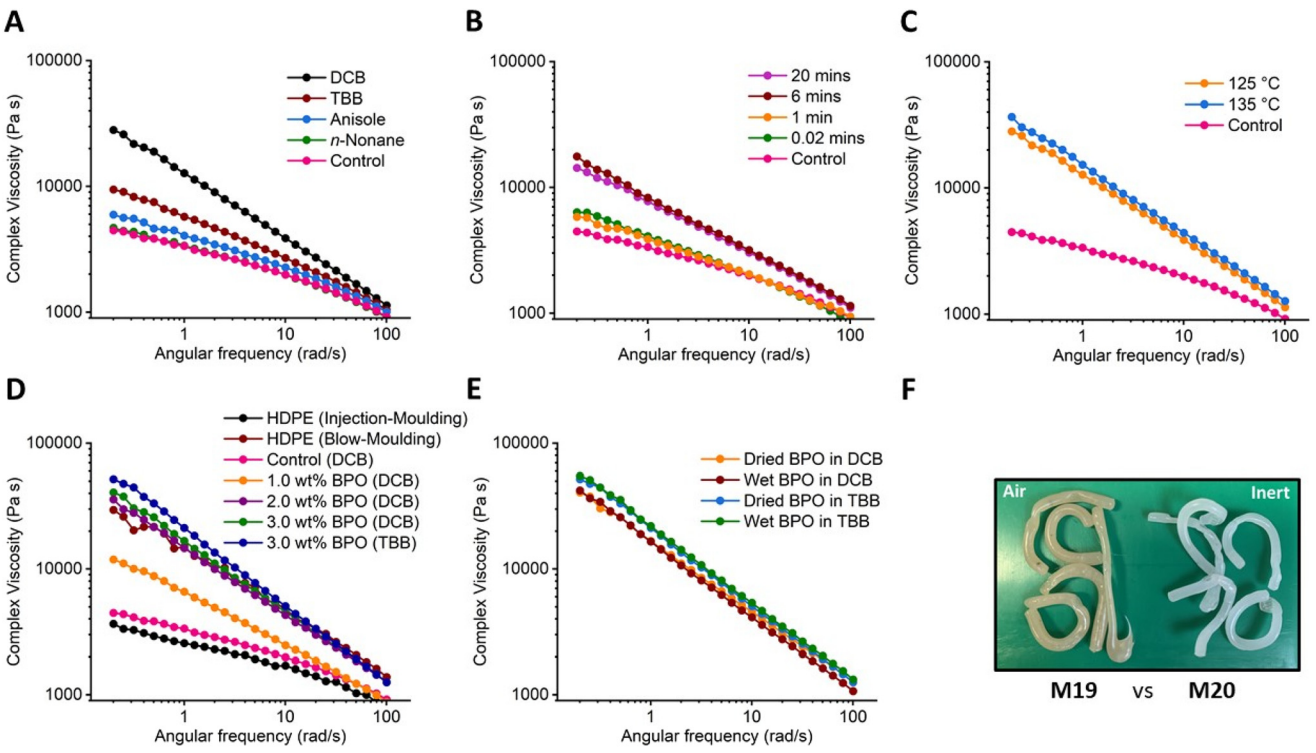


Fig. 5 Results from the experiments investigating the effects of changing (A) solvent, (B) peroxide addition duration, (C) reaction temperature, (D) peroxide, (E) water content and (F) oxygen presence in reaction medium.

*i.e.* can undergo side-reactions with the peroxide, especially when large quantities of solvent are present. It is worth noting that TBB has previously been used as a solvent for the peroxide-triggered grafting of maleic anhydride onto PE.[30] For anisole, the enhancement in polymer viscosity was relatively weak compared to DCB and TBB, yet it still surpassed the control, hinting at some chain extension albeit with some interference from the solvent reacting with the radical species. Sakurai *et al.* demonstrated that abstraction of a methyl proton from anisole is only slightly less favoured than that of toluene,[64] which has reactive benzylic protons due to resonance stabilisation of the resultant radical species. The readiness of anisole to undergo H-abstraction was attributed to the stabilisation of the resulting radical species through polar effects. Finally, the chain extension reactions performed in *n*-nonane did not show any enhancements in polymer melt viscosities. As this solvent can be considered as a polyethylene mimic, featuring multiple $CH_2$ repeat units, it is likely that *n*-nonane reacted with the generated radicals as it is present in the reaction vessel at much larger quantities (*vs.* only 7.5 w/v% IMPE).

To understand the impact of the rate of radical generation, investigations were performed altering the peroxide addition time and the reaction temperature (Fig. 5B and C). Firstly, the rate of adding the peroxide solution was reduced below 20 minutes to increase the maximum radical concentration in the solution. The results showed that adding the peroxide solution too quickly can reduce the extent of the chain modification reactions, where the addition of all of the peroxide over 1 min or in one-shot (~0.02 min) gave only a slightly enhanced viscosity profile compared to the control reaction (Fig. 5B). This could be because some of the generated radicals self-quench by reacting with each other. Increasing the reaction temperature by 10 °C did not result in a significant change in final polymer viscosity profiles at 4.5 wt% DLP loading (Fig. 5C).

To probe the influence of the peroxide, BPO was investigated as an alternative to DLP for the peroxide-triggered chain extension reactions. BPO is frequently used as an initiator in radical polymerisations; it is already produced in large quantities and is one of the most widely available and low-cost organic peroxides available. A series of experiments were performed with BPO in both DCB and TBB. As BPO is shock sensitive in its pure form, it is commonly sold as a 75% suspension in water, and it was dried at 40 °C under high vacuum overnight prior to these initial modification reactions (refer to Experimental for additional safety details). The results demonstrated that BPO is a strong chain modifier (Fig. 5D). Notably, both 2.0 and 3.0 wt% BPO loadings in DCB altered the viscosity profile of the injection-moulding grade polymer IMPE to blow-moulding grade PE. In addition, as BPO has a lower molecular weight (242.3 g $mol^{-1}$) than DLP (398.6 g $mol^{-1}$), lower quantities of the organic peroxide (in weight) are needed to achieve similar transformations. Given that DLP is 1.6 times heavier than BPO, DLP loadings of 3.0 and 4.5 wt% would correspond to ~2.0 and ~3.0 wt% BPO, respectively. Accordingly, it was shown that only 2.0 wt% BPO loading was enough to achieve the blow moulding grade transition, whereas 3.0 wt% DLP loading in DCB was not enough to obtain the same viscosity profile enhancement (Fig. 2, top). This difference hints that BPO may be a more suitable organic peroxide for the chain extension reactions. This may be because it releases radicals more slowly than DLP (the relative half-lives of DLP and BPO are 0.45 and 1.9 min in chlorobenzene), mirroring the reduced chain extension observed upon rapid addition of the peroxide (Fig. 5B). When a 3.0 wt% loading of BPO was used in TBB, instead of DCB, a strong viscosity enhancement was again observed by rheology. Interestingly, the viscosity enhancement was as significant (or even slightly more so) in TBB than DCB solvent, which differs from the result obtained using 4.5 wt% DLP loading (Fig. 5A), where the performance in TBB was significantly poorer than in DCB. This suggests that the reaction solvent can directly affect the organic peroxide decomposition and the subsequent chain extension reactions. These solvent effects are likely specific to each organic peroxide as the decomposition kinetics and/or mechanisms can be different.[65] SEC analysis was also performed (Fig. 6 and Table 3) on polymers modified with 3 wt% BPO in both DCB (**M15**) and TBB (**M16**). For both **M15** and **M16**, significantly higher $M_w$ values of 411 and 459 kg $mol^{-1}$ were obtained, respectively, compared to the control sample (**M1**, $M_w$ = 318 kg $mol^{-1}$). In addition, the dispersity values of both **M15** and **M16** were reported as 4.3, an increase from a dispersity of 3.2 for **M1**. The strong high molecular weight fronts are also clear in the overlay of the SEC chromatograms. Samples **M15** and **M16** were also tested using DSC (Fig. S105–108†) for the determination of their crystallinities. Similar to the earlier reported trends with DLP, the crystalli-

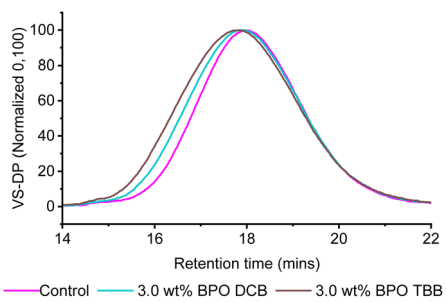


**Fig. 6** SEC viscometer traces recorded during the analysis of **M1**, **M15** and **M16**.

**Table 3** Molecular weight parameters of **M1**, **M15** and **M16** calculated using a conventional SEC calibration against polystyrene standards

| Exp. | Peroxide loading (wt%) | Solvent | $M_n$ (g $mol^{-1}$) | $M_w$ (g $mol^{-1}$) | $Đ$ |
|---|---|---|---|---|---|
| **M1** | 0 | DCB | 100 000 | 318 000 | 3.2 |
| **M15** | 3.0 | DCB | 95 000 | 411 000 | 4.3 |
| **M16** | 3.0 | TBB | 106 000 | 459 000 | 4.3 |

nities of **M15** and **M16** decreased to 63.7% and 62.5% (Table S2†), respectively.

Finally, the sensitivity of the modification reactions towards water and oxygen was investigated. As BPO was obtained as a 75% suspension in water from the supplier, wet BPO was used to test the sensitivity of the chain extension reaction to water in both DCB and TBB under a nitrogen atmosphere. The results demonstrated no significant sensitivity to water as the obtained complex viscosity profiles were almost identical (Fig. 5E), irrespective of whether wet or dry BPO was used. On the other hand, when the reactions were performed under air (**M19**), but in the absence of water, a discolouration of the reaction solution from colourless to pale yellow was observed, which was also reflected in the final polymer product (Fig. 5F). A deterioration in the polymer viscosity profile relative to both **M1** and **M20** was also observed (see ESI, Fig. S75†) as well as a clear indication of oxygenated moieties on the polymer backbone by NMR spectroscopy (Fig. 7). Indeed, the $^1$H NMR spectra revealed proton environments often attributed to aldehydes (~9.7 ppm) and other oxygenated moieties (3.0–5.0 ppm).[57] As oxygen is known to react with active radicals, it is believed to inhibit the LCB modification reactions (Scheme 1). Similar observations have been reported for radical polymerisations, where dead chain ends are generated in the presence of oxygen.[66] In support of these observations, where the system can tolerate water but not oxygen, atom-transfer radical polymerisations are often considered tolerant to alcohol groups and water as long as the reaction solution is deoxygenated prior to polymerisation.[67] It is worth noting that both **M19** and **M20** were prepared the same way and purified by precipitation into hexanes twice, and that far fewer oxygenated moieties were observed when the reaction was performed in the absence of oxygen (**M20**). In addition, a higher peroxide loading sample (**M5**, 6 wt% DLP) was also characterised using NMR spectroscopy and no strong signs of oxygenated species were detected. Yet even using just 0.5% peroxide loading in air showed oxygenated moieties (**M19**), indicating that these functional groups arise from the presence of air. Some studies have shown that oxygenated functional groups can enhance the polymer properties,[68] yet here, the presence of oxygenated moieties in **M19** clearly decreases the viscosity profiles, providing further support that the enhanced viscosity profiles are due to the presence of long chain branching.

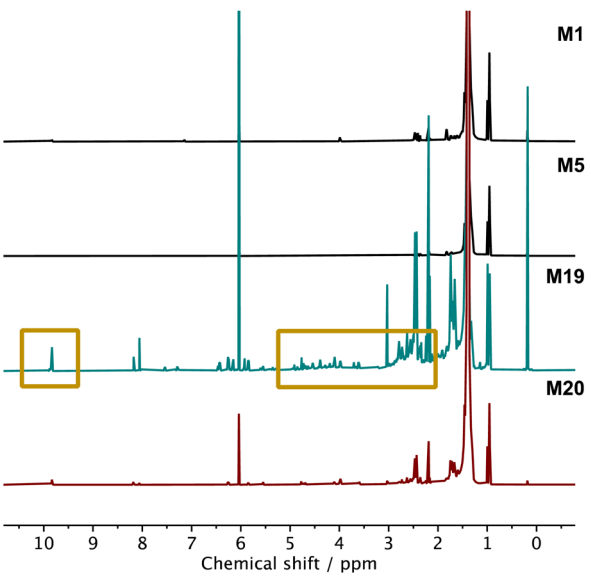


**Fig. 7** $^1$H NMR (800 MHz, 100 °C, $C_2D_2Cl_4$) spectra of **M1**, **M5**, **M19** and **M20**. The intensity of the main $CH_2$ peak at 1.4 ppm was normalised to 100 in all spectra to ensure a valid comparison.

### A model study

Chain extension reactions were further explored with a polyethylene-mimicking small molecule, *n*-dodecane, to understand how the modification reactions occur and provide insight into branching and the molecular weight increases. The solvent was changed to chlorobenzene as it has a lower boiling point than DCB (132 °C *vs.* 173 °C), to facilitate the separation of the solvent from *n*-dodecane and the reaction products (*e.g.*, *n*-dodecane, 216 °C). *n*-Dodecane was mixed in anhydrous chlorobenzene in a 1 : 1 weight ratio and degassed prior to the reaction. The alkane concentration was specifically chosen to be higher than the PE modification reactions, as the number of $CH_2$ units on *n*-dodecane is drastically lower than a HDPE chain. The temperature was then increased to 125 °C and a solution of pre-dried BPO in 1 ml chlorobenzene was added over a period of 20 min. Similar to the polymer modifications, the mixture was stirred for another 20 min before the reaction was terminated by cooling.

Characterisation of the reaction products was performed using SEC, where *n*-dodecane alone and the control experiment where no peroxide was present both gave a $M_n$ value of 180 g mol$^{-1}$ against polystyrene standards, which gives relatively good agreement with the molecular weight of *n*-dodecane being 170 g mol$^{-1}$ (Fig. 8A and Table 4). Following the peroxide-triggered modification reaction, the product gave a peak front as well as an increase in the overall $M_n$ value (230 g mol$^{-1}$), $M_w$ value (300 g mol$^{-1}$) and the dispersity ($Đ$ = 1.3). These results confirm that the modification reactions can extend the chain length of the starting material. In addition, analysing the product SEC trace as three separate peaks (Fig. 8B) showed that crude peak **(CP) 1** has $M_n$ (190 g mol$^{-1}$) similar to *n*-dodecane, while **CP2** and **CP3** had $M_n$ values of 340 g mol$^{-1}$ and 650 g mol$^{-1}$, respectively. **CP2** has a more distinctive peak shape, with an $M_n$ value approximately twice that obtained for *n*-dodecane (experimental values of 340 *vs.* 180 g mol$^{-1}$), which suggests it could be two *n*-dodecane chains linked together. On the other hand, **CP3** has a higher molecular weight hinting at multiple *n*-dodecane chains connected to each other, supported by the broad and poorly resolved peak shape. As the refractive index (RI) is a concentration detector, relative peak areas were also compared, and the results indicate that *n*-dodecane is the main species in the crude product, with higher molecular weight **CP2** being the second most dominant species.

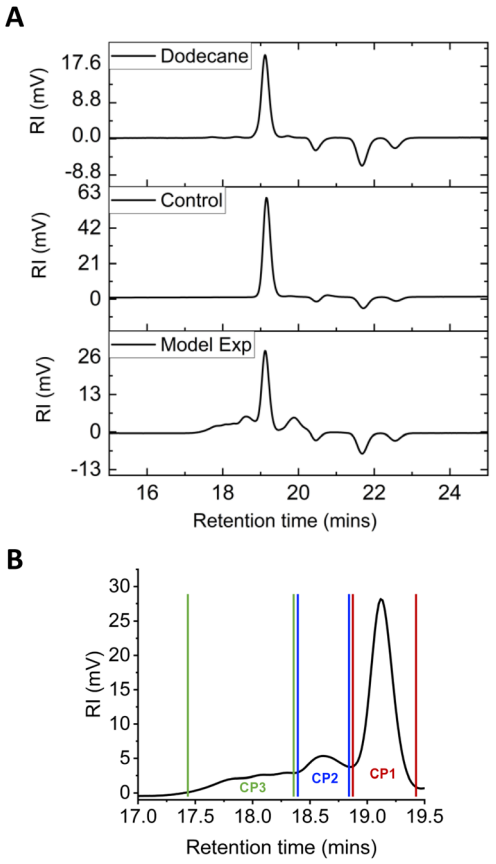


Fig. 8 (A) SEC traces recorded for dodecane (top), a control reaction with no peroxide (middle) and a model experiment performed with dried BPO, and (B) separation of the model product RI SEC trace into three separate peaks for conventional SEC analysis.

Table 4 Molecular weight parameters obtained from the model experiment using a conventional SEC calibration against polystyrene standards

| Sample | $M_n$ (g mol$^{-1}$) | $M_w$ (g mol$^{-1}$) | $Đ$ | RI peak area (%) |
|---|---|---|---|---|
| ***n*-Dodecane** | 180 | 180 | 1.0 | 100 |
| **Control** | 180 | 180 | 1.0 | 100 |
| **Model product** | 230 | 300 | 1.3 | 100 |
| **CP1** | 190 | 200 | 1.0 | 64 |
| **CP2** | 340 | 350 | 1.0 | 22 |
| **CP3** | 650 | 680 | 1.0 | 14 |

Further studies were also performed using NMR spectroscopy, where the model experiment crude product was placed under high vacuum to remove some of the unreacted dodecane. Characterisation of this sample revealed a new aliphatic-CH $^1$H NMR resonance at 1.40–1.75 ppm (Fig. S116†). This is notably different from the $^1$H NMR spectra of linear alkanes, which show diagnostic $CH_2$ resonances at 1.28–1.33 ppm, and $CH_3$ resonances at 0.89 ppm across a range of chain lengths (*e.g.* heptane, hexane, pentane, propane and ethane).[69,70] The new resonance at 1.40–1.75 ppm instead comes in a region associated with branched alkanes. Notably, the chemical shift of this CH resonance is significantly lower than that of oxygen-containing OCH units, which have chemical shifts around 3.5 ppm. Indeed, only trace resonances are present in the O–CH region of the spectrum. While there are other, aromatic resonances present in the $^1$H NMR spectrum, these are attributed to benzoic acid which is a common decomposition product of BPO, as both the $^1$H and $^{13}$C NMR spectra give good agreement with literature values.[71]

## Conclusions

To the best of our knowledge, this work presents the first solution-state methodology to modify HDPE by incorporating long chain PE branches through peroxide-based reactions. This strategy uses commercially available, low-cost organic peroxides and solvents, making the technology easily accessible. Both DLP and BPO are efficient peroxide modifiers, as long as they are used in solvents that do not significantly compete for H-abstraction compared to PE, such as DCB and TBB. The chain-extension has been confirmed through a variety of techniques including rheology, SEC and model studies based on *n*-dodecane as a small-molecule analogue of PE. The increased molecular weight is attributed to the incorporation of LCB, as rheological data shows the long chain branching index increases with increased DLP loading. Providing further support for the presence of LCB, the DSC and SAXS data confirm a loss of crystallinity with increased peroxide loading. All end products remained fully soluble suggesting homogeneous introduction of LCB throughout the polymer chains and demonstrating that no insoluble gel fractions were formed, which can be an issue with melt-phase peroxide modifications.

This study showcases the use of solution-state peroxide modification reactions as a simple method to enhance the material properties of HDPE from an injection moulding grade to a blow-moulding grade material. Furthermore, the data shows that the viscosity profiles can be tailored depending on the peroxide loading, potentially offering a facile route to modify the properties of PE for specific applications. This concept has the potential to be extended beyond PE, to the solution-state peroxide modification of other polymers. As higher molecular weight polymers with LCB are well-known to improve both the impact and chemical resistance of PE, this methodology could also offer a shortcut for the preparation of new PE grades and formulations with required specifications that may not currently be commercially available.

## Experimental

### Materials

IMPE (MFI – 4 g per 10 min at 190 °C, under 2.16 kg weight, Density – 948–952 kg m$^{-3}$ at 23 °C, Tensile modulus 1050–1150 MPa at 23 °C, 1 mm min$^{-1}$), BMPE – (MFI – 0.2 g per 10 min at 190 °C, under 2.16 kg weight, Density – 952–955 kg m$^{-3}$ at 23 °C, Tensile modulus 1000–1100 MPa at

23 °C, 100 mm $min^{-1}$). DLP (≥98%, Sigma-Aldrich) was used as received. BPO (72.0–77.0%, with 25% water, Sigma-Aldrich) was used as received or pre-dried *in vacuo* to remove water content (for reactions performed with dry BPO: see Safety notes). The solvents 1,2-DCB (99%, anhydrous, Sigma-Aldrich), TBB (99%, Sigma-Aldrich), anisole (99.7%, anhydrous, Sigma-Aldrich) and *n*-nonane (≥99%, anhydrous, Sigma-Aldrich) were dried over calcium hydride (95%, Sigma-Aldrich), then distilled and degassed prior to use. Xylenes (≥99%, Honeywell), hexanes (HPLC grade, 95% *n*-hexane, Fisher Scientific) and tetrachloroethane-$d_2$ (≥99.5 atom %D, Sigma-Aldrich) were used as received.

### Safety notes

All organic peroxides should be stored at temperatures below their self-accelerating decomposition temperature and as instructed by the supplier safety data sheet. BPO and acetone should never be mixed. Dry BPO is shock- and friction-sensitive, and can explode. Dried BPO was handled very carefully and dissolved in a compatible, anhydrous solvent for storage. Blast shields were used while adding the peroxide solutions into the hot reaction vessel. As organic peroxides can be incompatible with many chemicals, all reaction waste was tested for peroxide content using peroxide test strips. Peroxide testing indicated that all of the peroxide was consumed in the reactions reported here. In case the test returned a positive result, any leftover peroxide would need to be quenched. Any reactions that involved organic peroxides were disposed of using a separate waste stream. Tetrachloroethane-$d_2$ is extremely toxic and extra care must be taken when handling and disposing of this solvent. Sealed Young's tap NMR tubes were therefore used for NMR spectroscopic analysis.

### General procedure for modification reactions

IMPE (4.0 g) was placed into a pre-dried vessel and dried for 5 min under high vacuum, before filling the vessel with nitrogen. Then, anhydrous and degassed reaction solvent (60 ml) was injected into the reaction vessel before lowering it into a hot oil bath at 125 °C (or 135 °C for **M12**). The reaction mixture was stirred at this temperature for 60 min to dissolve the polymer. At the same time, an organic peroxide solution was prepared. The required amount of the organic peroxide (DLP, wet BPO or dry BPO) relative to the weight of the polymer (as stated in Table 1) was weighed into a vial and flushed with nitrogen for 5 min before adding the reaction solvent (1 ml) to dissolve the peroxide. It is important to note that wet-BPO was not soluble in TBB, and therefore DCB (1 ml) was used to prepare the peroxide solution for **M18**. The peroxide solution was stored in a suba seal secured vial until its use. The pre-prepared peroxide solution was then injected into the viscous polymer solution over the required number of minutes under $N_2$ atmosphere using a syringe pump. Following the addition, the reaction solution was stirred for an additional 20 min at reaction temperature before pouring it into hexanes to precipitate the polymer. The obtained powder was isolated by filtration and dissolved in xylenes (at 125 °C) before re-precipitating into hexanes. The final product was isolated by filtration and dried under dynamic vacuum for 4 hours at RT, before further drying by heating it to 150 °C for an additional 30 min under full vacuum.

### Model experiment

*n*-Dodecane (0.20 g, 1.2 mmol) was mixed with anhydrous chlorobenzene (0.22 ml) and degassed three times using freeze-pump thaw techniques, before heating the solution to 125 °C. At the same time, pre-dried BPO (20 mg, 0.083 mmol) was dissolved in anhydrous chlorobenzene (1 ml) and degassed under $N_2$ atmosphere. The peroxide solution was injected into the hot *n*-dodecane solution under $N_2$ atmosphere over 20 min. The final solution was then stirred for an additional 20 min at 125 °C, prior to lowering the temperature of the solution under running cold water tap (as *n*-dodecane and any other formed products were not expected to precipitate in hexanes). The solvent was removed *in vacuo* before characterising the sample with SEC.

### Rheology

Melt rheology of the PE samples was measured using a stress-controlled Kinexus Ultra+ rheometer (NETZSCH) with a 40 mm diameter 4° cone/plate tool with a 0.148 mm truncation gap. Oscillatory frequency sweeps were performed at 1% strain for all the samples ensuring that they remained in the linear viscoelastic regime. The frequency range for those experiments was from 0.01 to 16 Hz. Amplitude sweep tests were performed at 1 Hz and the strain was increased from 0.01 to 10%. All presented tests were performed at 190 °C unless otherwise noted; the temperature was controlled with a lower Peltier plate and active hood. Samples were prepared by direct melting on the lower plate and pressing with the upper geometry, samples were then allowed to relax to zero normal force. For semicrystalline polymers, such as the PE studied here, the large difference between the melt point and the glass transition restrict rheological measurements to the viscous regime and the low frequency cross-over.[28] Variation of the temperature from 140 to 200 °C, Fig. S11 and S30,† which does not significantly extend the measured viscoelastic reponse, confirms this. The validity of the Cox–Merz rule was established using shear start-up tests from 0.01 to 0.16 $s^{-1}$ over a strain of 10 and taking the final time-dependent viscosity to compare with the complex viscosity, Fig. S76 to S83.† Relaxation steps between each run were included to allow the sample to relax (500 to 1000 s). Shear start-up tests for the samples used a 20 mm diameter parallel plate at a gap of 0.5 mm.

### Melt flow index analysis

Melt flow index values were determined according to the ISO 1133 standard protocol. Between 2–8 g of polyethylene was charged into the barrel of the machine, where the material was preheated for 5 minutes. The test was completed at 190 °C ± 0.5 °C for polyethylene and melt flow was measured using a 2.16 kg weight. Three cuts of the polyethylene extrudate were

 

obtained in three set time periods. The average was taken, and the results are reported in g per 10 minutes. Note: the mass of polymer sample and the time intervals between cuts were determined by the MFI of the material being run.

### Size exclusion chromatography

Molecular weight and dispersity values of the modified PE samples were determined using an Agilent 1260 Infinity II HT-GPC/SEC system through Agilent PLgel Mixed-C columns. The SEC characterisation was performed in butylal at 150 °C with a flow rate of 1.00 ml $min^{-1}$. SEC characterisation of the model study results was performed using an Agilent 1260 Infinity II multidetector GPC/SEC system through PLgel 5 μm columns packed with polystyrene-divinylbenzene beads, in tetrahydrofuran at 35 °C with a flow rate of 1.00 ml $min^{-1}$. All SEC calibrations were obtained using narrow dispersity polystyrene standards.

### NMR spectroscopy

All PE samples were dissolved in tetrachloroethane-$d_2$ at 125 °C. The sample concentrations were kept at ~25 mg $ml^{-1}$. All 1D NMR data were obtained at 100 °C using a Bruker Neo spectrometer operating at 799.57 MHz ($^1$H frequency) equipped with triple-resonance TXO 13C/15N optimised cryoprobe. Due to the toxicity of the NMR solvent, the samples were analysed in Young's tap NMR tubes.

### Differential scanning calorimetry

The measurements were carried out on a DSC 2500 TA instrument using a heat (30–200 °C)/cool (200–30 °C)/heat (30–200 °C) cycle at a rate of 10 °C $min^{-1}$, unless otherwise stated. Values of enthalpy changes and crystallinities were obtained from the second heating scan.

### SAXS/WAXS analysis

Samples were prepared by melting and pressing each polymer between two hot glass slides to form thin polymer films of approximately ~0.5 mm in thickness. Scattering patterns were recorded at a synchrotron facility (ESRF, beamline ID02, Grenoble, France)[72] using a monochromatic X-ray source wavelength $\lambda$ = 0.0995 nm, with $q$ ranging from 0.021 to 2.9 $nm^{-1}$ for SAXS, and from 7.8 to 34.9 $nm^{-1}$ wide angle X-ray scattering or WAXS, where $q$ is the length of the scattering vector (*i.e.*, $q = (4\pi/\lambda)\sin\theta$, and $\theta$ is the half of the scattering angle), and a Ravonix MX-170HS CCD detector. The precise thickness of the polymer films were measured and then they were mounted in transmission mode with respect to the X-ray beam. Scattering data were reduced using standard routines from the beamline,[72] and were further analysed using SAXS utilities and Origin software, where the intensity of the signals was corrected for film thickness. Specifically, the degree of crystallinity was calculated using Origin software and was determined by the ratio of the integrals between the crystalline and amorphous peaks.

## Author contributions

J. A. G. and U. Y. designed the project. U. Y. and T. J. N. performed the experiments. U. Y., J. A. R. and J. R. R. designed the rheological tests. U. Y, T. J. N and J. A. R. wrote the manuscript. J. A. G. and J. R. R. edited the manuscript. J. A. G. acquired the funding and directed the research.

## Conflicts of interest

There are no conflicts to declare.

## Acknowledgements

This work was supported by InnovateUK (10018521), UKRI and the Henry Royce Institute for Advanced Materials, funded through EPSRC grants EP/R00661X/1, EP/S019367/1, EP/P025021/1 and EP/P025498/1, as well as the UKRI Future Leaders Fellowship (Grant MR/T042710/1). We gratefully acknowledge the University of Edinburgh NMR facility team (Dr Juraj Bella and Dr Lorna Murray) as well as the Henry Royce Institute Chemical Materials Design team (Matthew Hutchins) for their help in characterising the reported polymers. Finally, we would like to thank Monica Chandwani and Hannah Logan for DSC instrument training and UK Ministry of Defence for funding the equipment. The authors are grateful to ESRF (Grenoble, France) for providing SAXS beam-time (experiment SC5315), and the personnel of the ID02 station are thanked for help with the synchrotron measurements.

## References

1 R. W. Nunes, J. R. Martin and J. F. Johnson, Influence of molecular weight and molecular weight distribution on mechanical properties of polymers, *Polym. Eng. Sci.*, 1982, **22**, 205–228.
2 W. G. Perkins, N. J. Capiati and R. S. Porter, The effect of molecular weight on the physical and mechanical properties of ultra-drawn high density polyethylene, *Polym. Eng. Sci.*, 1976, **16**, 200–203.
3 H. G. Hester, B. A. Abel and G. W. Coates, Ultra-High-Molecular-Weight Poly(Dioxolane): Enhancing the Mechanical Performance of a Chemically Recyclable Polymer, *J. Am. Chem. Soc.*, 2023, **145**, 8800–8804.
4 C. I. Simionescu, B. C. Simionescu and S. Ioan, Plasma-Induced Living Radical Copolymerization, *J. Macromol. Sci., Part A*, 1985, **22**, 765–778.
5 Y. Kamiyama, R. Tamate, T. Hiroi, S. Samitsu, K. Fujii and T. Ueki, Highly stretchable and self-healable polymer gels from physical entanglements of ultrahigh–molecular weight polymers, *Sci. Adv.*, 2022, **8**, eadd0226.
6 K. Patel, S. H. Chikkali and S. Sivaram, Ultrahigh molecular weight polyethylene: Catalysis, structure, properties, processing and applications, *Prog. Polym. Sci.*, 2020, **109**, 101290.

7 M. L. Lepage, C. Simhadri, C. Liu, M. Takaffoli, L. Bi, B. Crawford, A. S. Milani and J. E. Wulff, A broadly applicable cross-linker for aliphatic polymers containing C–H bonds, *Science*, 2019, **366**, 875–878.
8 H. Ahmad and D. Rodrigue, Crosslinked polyethylene: A review on the crosslinking techniques, manufacturing methods, applications, and recycling, *Polym. Eng. Sci.*, 2022, **62**, 2376–2401.
9 J.-P. Pascault and R. J. J. Williams, in *Handbook of Polymer Synthesis, Characterization, and Processing*, 2013, pp. 519–533, DOI: **10.1002/9781118480793.ch28**.
10 R. Geyer, J. R. Jambeck and K. L. Law, Production, use, and fate of all plastics ever made, *Sci. Adv.*, 2017, **3**, e1700782.
11 Y.-F. Huang, J.-Z. Xu, J.-Y. Xu, Z.-C. Zhang, B. S. Hsiao, L. Xu and Z.-M. Li, Self-reinforced polyethylene blend for artificial joint application, *J. Mater. Chem. B*, 2014, **2**, 971–980.
12 K. Ishihara, Highly lubricated polymer interfaces for advanced artificial hip joints through biomimetic design, *Polym. J.*, 2015, **47**, 585–597.
13 T. Röding, J. Langer, T. Modenesi Barbosa, M. Bouhrara and T. Gries, A review of polyethylene-based carbon fiber manufacturing, *Appl. Res.*, 2022, **1**, e202100013.
14 Z. Wang, Q. Mahmood, W. Zhang and W.-H. Sun, in *Advances in Organometallic Chemistry*, ed. P. J. Pérez, Academic Press, 2023, vol. 79, pp. 41–86.
15 Q. Mahmood and W.-H. Sun, N,N-chelated nickel catalysts for highly branched polyolefin elastomers: a survey, *R. Soc. Open Sci.*, 2018, **5**, 180367.
16 Z. Wang, Q. Liu, G. A. Solan and W.-H. Sun, Recent advances in Ni-mediated ethylene chain growth: Nimine-donor ligand effects on catalytic activity, thermal stability and oligo-/polymer structure, *Coord. Chem. Rev.*, 2017, **350**, 68–83.
17 A. I. Moncada, W. Huang and N. Horstman, in *Handbook of Industrial Polyethylene and Technology*, 2017, pp. 715–749, DOI: **10.1002/9781119159797.ch24**.
18 D. Suwanda and S. T. Balks, The reactive modification of polyethylene. I: The effect of low initiator concentrations on molecular properties, *Polym. Eng. Sci.*, 1993, **33**, 1585–1591.
19 C. Meola, G. M. Carlomagno and G. Giorleo, in *Encyclopedia of Chemical Processing*, ed. S. Lee, Taylor and Francis, 1 edn, 2006, pp. 577–588.
20 K. S. Whiteley, T. G. Heggs, H. Koch, R. L. Mawer and W. Immel, in *Ullmann's Encyclopedia of Industrial Chemistry*, 2000, DOI: **10.1002/14356007.a21_487**.
21 Z. O. G. Schyns and M. P. Shaver, Mechanical Recycling of Packaging Plastics: A Review, *Macromol. Rapid Commun.*, 2021, **42**, 2000415.
22 D. Akbarian, H. Hamedi, B. Damirchi, D. E. Yilmaz, K. Penrod, W. H. H. Woodward, J. Moore, M. T. Lanagan and A. C. T. van Duin, Atomistic-scale insights into the crosslinking of polyethylene induced by peroxides, *Polymer*, 2019, **183**, 121901.
23 J. Vega, M. Aguilar, J. Peón, D. Pastor and J. Martínez-Salazar, Effect of long chain branching on linear-viscoelastic melt properties of polyolefins, *e-Polymers*, 2002, **2**(1), 45–80.
24 Y. C. Kim and K. S. Yang, Effect of Peroxide Modification on Melt Fracture of Linear Low Density Polyethylene during Extrusion, *Polym. J.*, 1999, **31**, 579–584.
25 Y. Tang, C. Tzoganakis, A. E. Hamielec and J. Vlachopoulos, Peroxide crosslinking of LLDPE during reactive extrusion, *Adv. Polym. Technol.*, 1989, **9**, 217–226.
26 P. S. M. Cardoso, M. M. Ueki, J. D. V. Barbosa, F. C. Garcia Filho, B. S. Lazarus and J. B. Azevedo, The Effect of Dialkyl Peroxide Crosslinking on the Properties of LLDPE and UHMWPE, *Polymers*, 2021, **13**, 3062–3077.
27 H. B. Parmar, R. K. Gupta and S. N. Bhattacharya, Melt Strength and Thermal Properties of Organic Peroxide Modified Virgin and Recycled HDPE, *Int. Polym. Process.*, 2008, **23**, 200–207.
28 S. L. Morelly and N. J. Alvarez, Characterizing long-chain branching in commercial HDPE samples via linear viscoelasticity and extensional rheology, *Rheol. Acta*, 2020, **59**, 797–807.
29 E. M. Kampouris and A. G. Andreopoulos, Gel content determination in cross-linked polyethylene, *Biomaterials*, 1989, **10**, 206–208.
30 A. Priola, R. Bongiovanni and G. Gozzelino, Solvent influence on the radical grafting of maleic anhydride on low density polyethylene, *Eur. Polym. J.*, 1994, **30**, 1047–1050.
31 R. L. Eagan and L. K. Templeton, WO 02/34801 A1, 2002.
32 D. B. Malpass, *Introduction to Polymers of Ethylene*, Wiley, 2010.
33 H. Sinn and W. Kaminsky, in *Advances in Organometallic Chemistry*, ed. F. G. A. Stone and R. West, Academic Press, 1980, vol. 18, pp. 99–149.
34 B. Pelzl, R. Wolf and B. L. Kaul, in *Ullmann's Encyclopedia of Industrial Chemistry*, 2018, pp. 1–57, DOI: **10.1002/14356007.a20_459.pub2**.
35 M. Uhniat and S. Kudła, Stabilisation of LDPE cross-linked in the presence of peroxides I. Kinetic study of the oxidation, *Polym. Degrad. Stab.*, 2000, **71**, 69–74.
36 S. Al-Malaika, S. Riasat and C. Lewucha, Reactive antioxidants for peroxide crosslinked polyethylene, *Polym. Degrad. Stab.*, 2017, **145**, 11–24.
37 I. Chodák, A. Romanov, M. Rätzsch and G. Haudel, Influence of the additives on polyethylene crosslinking initiated by peroxides, *Acta Polym.*, 1987, **38**, 672–674.
38 H. A. Khonakdar, Branching degree and rheological response correlation in peroxide-modified linear low-density polyethylene, *Polym. Adv. Technol.*, 2014, **25**, 835–841.
39 F. Wu, M. Misra and A. K. Mohanty, Super Toughened Poly (lactic acid)-Based Ternary Blends via Enhancing Interfacial Compatibility, *ACS Omega*, 2019, **4**, 1955–1968.
40 Nouryon, Product Data Sheets, **https://www.nouryon.com/globalassets/inriver/resources/pds-laurox-w-40-polymer-production-glo-en.pdf** and **https://www.nouryon.com/globalassets/inriver/resources/pds-perkadox-l-w75-powder-usp-**

grade-pharmaceutical-industry-glo-en.pdf, (accessed 04/2023).
41 W. P. Cox and E. H. Merz, Correlation of dynamic and steady flow viscosities, *J. Polym. Sci.*, 1958, **28**, 619–622.
42 J. D. Ferry, *Viscoelastic Properties of Polymers*, Wiley, 1970.
43 M. Rubinstein and R. H. Colby, *Polymer Physics*, OUP, Oxford, 2003.
44 J. Vlachopoulos and N. Polychronopoulos, in *Applied Polymer Rheology*, 2011, pp. 1–27, DOI: 10.1002/9781118140611.ch1.
45 C. Erbetta, G. Manoel, A. Oliveira, M. Silva, R. Freitas and R. Sousa, Rheological and thermal behavior of high-density polyethylene (HDPE) at different temperatures, *Mater. Sci. Appl.*, 2014, **5**, 923–931.
46 D. Yan, W. J. Wang and S. Zhu, Effect of long chain branching on rheological properties of metallocene polyethylene, *Polymer*, 1999, **40**, 1737–1744.
47 A. Shrivastava, in *Introduction to Plastics Engineering*, ed. A. Shrivastava, William Andrew Publishing, 2018, pp. 17–48, DOI: 10.1016/B978-0-323-39500-7.00002-2.
48 J. P. Greene, in *Automotive Plastics and Composites*, ed. J. P. Greene, William Andrew Publishing, 2021, pp. 27–37, DOI: 10.1016/B978-0-12-818008-2.00009-X.
49 N. P. Bessonova, S. V. Krasheninnikov, M. A. Shcherbina and S. N. Chvalun, Thermal behavior of crystalline and amorphous HDPE phase in the process of necking at creep deformation, *Polym. Test.*, 2021, **97**, 107127.
50 L. A. Pruitt, in *Comprehensive Biomaterials*, ed. P. Ducheyne, Elsevier, Oxford, 2011, pp. 373–379, DOI: 10.1016/B978-0-08-055294-1.00036-2.
51 K. J. Tanaka, The Effect of Chain Branching and Molecular Weight of Polyethylene on its Glass Transition Temperature, *Bull. Chem. Soc. Jpn.*, 1960, **33**, 1133–1137.
52 A. Romo-Uribe, A. Manzur and R. Olayo, Synchrotron small-angle x-ray scattering study of linear low-density polyethylene under uniaxial deformation, *J. Mater. Res.*, 2012, **27**, 1351–1359.
53 M. F. Butler, A. M. Donald, W. Bras, G. R. Mant, G. E. Derbyshire and A. J. Ryan, A Real-Time Simultaneous Small- and Wide-Angle X-ray Scattering Study of In-Situ Deformation of Isotropic Polyethylene, *Macromolecules*, 1995, **28**, 6383–6393.
54 A. J. Ryan, W. Bras, G. R. Mant and G. E. Derbyshire, A direct method to determine the degree of crystallinity and lamellar thickness of polymers: application to polyethylene, *Polymer*, 1994, **35**, 4537–4544.
55 T. Nedkov, F. Lednický and M. Mihailova, Compatibilization of PP/PE blends and scraps with Royalene: Mechanical properties, SAXS, and WAXS, *J. Appl. Polym. Sci.*, 2008, **109**, 226–233.
56 F. Cser, About the Lorentz correction used in the interpretation of small angle X-ray scattering data of semicrystalline polymers, *J. Appl. Polym. Sci.*, 2001, **80**, 2300–2308.
57 J. C. Randall, A Review of High Resolution Liquid 13Carbon Nuclear Magnetic Resonance Characterizations of Ethylene-Based Polymers, *J. Macromol. Sci., Part C*, 1989, **29**, 201–317.
58 P. M. Wood-Adams and J. M. Dealy, Using Rheological Data To Determine the Branching Level in Metallocene Polyethylenes, *Macromolecules*, 2000, **33**, 7481–7488.
59 P. M. Wood-Adams, J. M. Dealy, A. W. deGroot and O. D. Redwine, Effect of Molecular Structure on the Linear Viscoelastic Behavior of Polyethylene, *Macromolecules*, 2000, **33**, 7489–7499.
60 Z. Zhou, C. Anklin, R. Cong, X. Qiu and R. Kuemmerle, Long-Chain Branch Detection and Quantification in Ethylene–Hexene LLDPE with $^{13}$C NMR, *Macromolecules*, 2021, **54**, 757–762.
61 R. L. Bennett, A. Keller and J. Stejny, Study of the direct detection of crosslinks in hydrocarbons by 13C-NMR. I. Preparation and characterization of model compound 1,1,2,2-tetra(tridecyl) ethane, *J. Polym. Sci., Polym. Chem. Ed.*, 1976, **14**, 3021–3026.
62 J. C. Randall, in *Crosslinking and Scission in Polymers*, ed. O. Güven, Springer Netherlands, Dordrecht, 1990, pp. 57–82, DOI: 10.1007/978-94-009-1924-2_4.
63 Q. Zhu, F. Horil, R. Kitamaru and H. Yamaoka, 13C-NMR study of crosslinking and long-chain branching in linear polyethylene induced by 60Co gamma ray irradiation at different temperatures, *J. Polym. Sci., Part A: Polym. Chem.*, 1990, **28**, 2741–2751.
64 H. Sakurai, A. Hosomi and M. Kumada, Abstraction of methyl hydrogen of substituted anisoles by tert-butoxy radicals, *J. Org. Chem.*, 1970, **35**, 993–996.
65 P. D. Bartlett and K. Nozaki, The Decomposition of Benzoyl Peroxide in Solvents. II. Ethers, Alcohols, Phenols and Amines, *J. Am. Chem. Soc.*, 1947, **69**, 2299–2306.
66 R. Simič, J. Mandal, K. Zhang and N. D. Spencer, Oxygen inhibition of free-radical polymerization is the dominant mechanism behind the "mold effect" on hydrogels, *Soft Matter*, 2021, **17**, 6394–6403.
67 K. Matyjaszewski, in *Encyclopedia of Materials: Science and Technology*, eds. K. H. J. Buschow, R. W. Cahn, M. C. Flemings, B. Ilschner, E. J. Kramer, S. Mahajan and P. Veyssière, Elsevier, Oxford, 2001, pp. 356–365, DOI: 10.1016/B0-08-043152-6/00073-5.
68 J. X. Shi, N. R. Ciccia, S. Pal, D. D. Kim, J. N. Brunn, C. Lizandara-Pueyo, M. Ernst, A. M. Haydl, P. B. Messersmith, B. A. Helms and J. F. Hartwig, Chemical Modification of Oxidized Polyethylene Enables Access to Functional Polyethylenes with Greater Reuse, *J. Am. Chem. Soc.*, 2023, **145**, 21527–21537.
69 N. R. Babij, E. O. McCusker, G. T. Whiteker, B. Canturk, N. Choy, L. C. Creemer, C. V. D. Amicis, N. M. Hewlett, P. L. Johnson, J. A. Knobelsdorf, F. Li, B. A. Lorsbach, B. M. Nugent, S. J. Ryan, M. R. Smith and Q. Yang, NMR Chemical Shifts of Trace Impurities: Industrially Preferred Solvents Used in Process and Green Chemistry, *Org. Process Res. Dev.*, 2016, **20**, 661–667.
70 G. R. Fulmer, A. J. M. Miller, N. H. Sherden, H. E. Gottlieb, A. Nudelman, B. M. Stoltz, J. E. Bercaw and K. I. Goldberg, NMR Chemical Shifts of Trace Impurities: Common Laboratory Solvents, Organics, and Gases in Deuterated

Solvents Relevant to the Organometallic Chemist, *Organometallics*, 2010, **29**, 2176–2179.
71 Y. Zhang, Y. Cheng, H. Cai, S. He, Q. Shan, H. Zhao, Y. Chen and B. Wang, Catalyst-free aerobic oxidation of aldehydes into acids in water under mild conditions, *Green Chem.*, 2017, **19**, 5708–5713.
72 T. Narayanan, M. Sztucki, P. Van Vaerenbergh, J. Léonardon, J. Gorini, L. Claustre, F. Sever, J. Morse and P. Boesecke, A multipurpose instrument for time-resolved ultra-small-angle and coherent X-ray scattering, *J. Appl. Crystallogr.*, 2018, **51**, 1511–1524.